Calvin Cycle Flux, Pathway Constraints, and Substrate Oxidation State Together Determine the H_2 Biofuel Yield in Photoheterotrophic Bacteria

James B. McKinlay and Caroline S. Harwood

Department of Microbiology, University of Washington, Seattle, Washington, USA

ABSTRACT **Hydrogen gas (H_2) is a possible future transportation fuel that can be produced by anoxygenic phototrophic bacteria via nitrogenase. The electrons for H_2 are usually derived from organic compounds. Thus, one would expect more H_2 to be produced when anoxygenic phototrophs are supplied with increasingly reduced (electron-rich) organic compounds. However, the H_2 yield does not always differ according to the substrate oxidation state. To understand other factors that influence the H_2 yield, we determined metabolic fluxes in *Rhodopseudomonas palustris* grown on ^{13}C-labeled fumarate, succinate, acetate, and butyrate (in order from most oxidized to most reduced). The flux maps revealed that the H_2 yield was influenced by two main factors in addition to substrate oxidation state. The first factor was the route that a substrate took to biosynthetic precursors. For example, succinate took a different route to acetyl-coenzyme A (CoA) than acetate. As a result, *R. palustris* generated similar amounts of reducing equivalents and similar amounts of H_2 from both succinate and acetate, even though succinate is more oxidized than acetate. The second factor affecting the H_2 yield was the amount of Calvin cycle flux competing for electrons. When nitrogenase was active, electrons were diverted away from the Calvin cycle towards H_2, but to various extents, depending on the substrate. When Calvin cycle flux was blocked, the H_2 yield increased during growth on all substrates. In general, this increase in H_2 yield could be predicted from the initial Calvin cycle flux.**

IMPORTANCE **Photoheterotrophic bacteria, like *Rhodopseudomonas palustris*, obtain energy from light and carbon from organic compounds during anaerobic growth. Cells can naturally produce the biofuel H_2 as a way of disposing of excess electrons. Unexpectedly, feeding cells organic compounds with more electrons does not necessarily result in more H_2. Despite repeated observations over the last 40 years, the reasons for this discrepancy have remained unclear. In this paper, we identified two metabolic factors that influence the H_2 yield, (i) the route taken to make biosynthetic precursors and (ii) the amount of CO_2-fixing Calvin cycle flux that competes against H_2 production for electrons. We show that the H_2 yield can be improved on all substrates by using a strain that is incapable of Calvin cycle flux. We also contributed quantitative knowledge to the long-standing question of why photoheterotrophs must produce H_2 or fix CO_2 even on relatively oxidized substrates.**

Received 5 December 2010 **Accepted** 15 February 2011 **Published** 22 March 2011

Citation McKinlay JB, Harwood CS. 2011. Calvin cycle flux, pathway constraints, and substrate oxidation state together determine the H_2 biofuel yield in photoheterotrophic bacteria. mBio 2(2):e00323-10. doi:10.1128/mBio.00323-10.

Editor Dianne Newman, California Institute of Technology

Address correspondence to Caroline S. Harwood, csh5@uw.edu.

Hydrogen gas (H_2) is a promising transportation fuel that can be used in hydrogen fuel cells to generate an electric current with water as the only waste product. Anoxygenic phototrophic bacteria, including purple nonsulfur bacteria (PNSB), produce H_2 via nitrogenase (1). H_2 production is an obligate product of the nitrogenase reaction, which is better known for converting N_2 gas to NH_3. In fact, nitrogenase will produce H_2 as the sole product in the absence of N_2. To invoke H_2 production, PNSB are grown under conditions that induce nitrogenase activity, such as by supplying N_2, or in some cases glutamate, as the sole nitrogen source (2–5). Also, several PNSB mutants have been identified that produce H_2 when grown with NH_4^+ as a nitrogen source, a condition that normally represses nitrogenase synthesis (4, 6–8). These mutants typically have activating mutations in *nifA*, encoding the master transcriptional activator of nitrogenase, and are termed NifA* strains (4, 6, 7).

The preferred mode of growth for PNSB is photoheterotrophy, where light provides energy by photophosphorylation and organic compounds are used for carbon. In a recent study, we found that *Rhodopseudomonas palustris* cells grown with ^{13}C-labeled acetate incorporated most of the acetate into cell material but that only half of the reducing equivalents that were generated during acetate oxidation were used in biosynthetic reactions. The bacteria were required to oxidize the other half of the reduced carriers of reducing equivalents (e.g., NADH, NADPH, and ferredoxins, here collectively referred to as electron carriers) by some other means. In the case of acetate, cells accomplished this by carrying out CO_2 fixation via the Calvin cycle or by producing H_2 (7). Others have shown that the Calvin cycle is essential during photoheterotrophic growth on other substrates, even substrates that are substantially more oxidized than biomass (9, 10). PNSB mutants lacking the CO_2-fixing enzyme of the Calvin cycle, ribulose

1,5-bisphosphate carboxylase (RuBisCO), were unable to grow on malate, succinate, or acetate unless cells were grown under nitrogen-fixing conditions to allow H_2 production (7, 11) or unless the electron acceptor dimethyl sulfoxide was provided (9, 10).

Given the important role for H_2 production in oxidizing electron carriers, one would expect PNSB to produce more H_2 from more-reduced substrates and less H_2 from more-oxidized substrates. However, it has long been known that H_2 yields from PNSB do not always differ accordingly with the substrate oxidation state. In 1977, Hillmer and Gest reported that *Rhodobacter capsulatus* produced about twice as much H_2 from pyruvate as from glucose, a more reduced substrate (2). Similar results have been reported for other PNSB (3, 5). One factor that certainly affects H_2 yields from different substrates is the amounts of storage products, such as polyhydroxybutyrate, and excreted organic acids produced (5, 12). H_2 yields from *Rhodobacter sphaeroides* also appeared to correlate with the substrate free energy (5), a surprising result given that H_2 production is not expected to be limited by energy during photosynthetic growth.

To identify factors other than substrate oxidation state that influence H_2 production, we performed ^{13}C metabolic flux analysis with *R. palustris* provided with organic compounds with a range of oxidation states. We determined metabolic fluxes for the wild type (WT) and a NifA* strain grown anaerobically in light in mineral medium containing NH_4^+ as the nitrogen source. The wild-type strain does not produce H_2 under these conditions, whereas the NifA* strain expresses nitrogenase and produces H_2 constitutively. This comparison allowed us to determine the contribution of the Calvin cycle to the growth obtained when nitrogenase is not present compared to the growth obtained when nitrogenase is active and competing against the Calvin cycle for electrons by producing H_2. Our results illustrate how the biochemical constraints of a metabolic network can affect the H_2 yield when meeting demands for biosynthetic precursors. Our results also show that Calvin cycle activity decreases to different extents, depending on the organic substrate supplied, thereby affecting the H_2 yield by competing for electrons.

RESULTS

H_2 yields and characteristics of growth on different substrates. Previous reports with various PNSB indicated that H_2 yields do not always differ according to the substrate oxidation state (2, 3, 5). To confirm this, we determined the H_2 yields from *R. palustris* grown on unlabeled substrates with various oxidation states that were also available in ^{13}C-labeled forms (Table 1). To achieve H_2 production, we used a NifA* strain that synthesizes active nitrogenase in mineral medium containing NH_4^+. The wild-type strain does not synthesize nitrogenase and produces no H_2 when grown in this medium. Fumarate, succinate, and acetate all gave similar H_2 yields despite differing in oxidation state (Table 1). The most H_2 was produced during growth on the most reduced substrate, butyrate.

We accounted for nearly all of the consumed carbon and electrons in biomass, CO_2, H_2, and excreted organic acids (Table 2). As expected (13), growth on butyrate, a compound more reduced than biomass, required $NaHCO_3$ unless H_2 was produced (Table 2). In all cases, more CO_2 was produced by the NifA* strain than by the wild type, consistent with electrons being shifted away from CO_2 fixation towards H_2 production. This is reflected in lower biomass yields for the NifA* strain (Table 2).

TABLE 1 Oxidation states of *R. palustris* biomass and growth substrates and the H_2 yield from each substrate

Compound	Formula	Oxidation state[b]	H_2 yield (mol H_2/100 mol organic C consumed)[c]
Fumarate	$C_4H_4O_4$	+1	18 ± 3[d]
Succinate	$C_4H_6O_4$	+0.5	23 ± 1
Acetate	$C_2H_4O_2$	0	21 ± 3
Biomass[a]	$CH_{1.8}N_{0.18}O_{0.38}$	−0.5	
Butyrate	$C_4H_8O_2$	−1	41 ± 10

[a] Based on the elemental composition of *R. palustris* 42OL (25).
[b] Values were determined for each carbon atom as described previously (7, 26) and then averaged by dividing the sum by the number of carbon atoms.
[c] NifA* cultures were grown in minimal medium with NH_4^+ as the nitrogen source. Values are averages from 3 to 5 biological replicates ± standard deviations (SD) based on samples taken during early exponential growth. Values are normalized for organic C consumed to account for the different carbon contents between acetate and the other substrates.
[d] Calculated by grouping fumarate and malate as a single metabolite [i.e., $d$$H_2$/$d$(fumarate + malate) × 100/4 carbon atoms]. The H_2 yield from fumarate consumed alone would give a value of 12 ± 2.

Whereas acetate was converted entirely into CO_2 and biomass, growth on all other substrates resulted in organic acid excretion (Table 2). A relatively large proportion of fumarate was excreted as malate (growth on malate also resulted in fumarate excretion), a relatively large proportion of butyrate was excreted as acetate, and a small proportion of succinate was excreted as fumarate. For all substrates, excreted organic acids were eventually consumed. Since fumarate and malate have the same oxidation state, we grouped them as one metabolite to account for their simultaneous consumption and to better reflect the effects of intermediary metabolic fluxes on H_2 yield. If we were to show the H_2 yield as a proportion of fumarate consumed alone, without accounting for reconsumption of malate, then the H_2 yield would be deceptively low. We did not group butyrate and acetate, since these compounds have different oxidation states and thus acetate excretion informs us about fluxes that reduce electron carriers.

R. palustris showed typical exponential growth curves on all substrates except for fumarate. Growth on fumarate was biphasic, with rapid growth (i.e., 5.8 ± 0.3 h for the wild type and 6.4 ± 0.5 h for the NifA* strain) before a cell density of about 0.06 units of optical density at 660 nm (OD_{660}) was reached, followed by a lower growth rate (Table 2) that lasted for the remainder of exponential growth. ^{13}C metabolic flux analysis is based on equations that describe a metabolic steady state (or a pseudometabolic steady state in batch cultures). Therefore, our flux maps for biphasic fumarate-grown cultures may not be quantitatively accurate. However, the majority of the labeling patterns (~85%) accumulated during the second exponential growth phase. Thus, the statements about fluxes on fumarate relative to other substrates should be qualitatively accurate.

The Calvin cycle is important for maintaining electron balance on all substrates. After confirming that cells convert the compounds provided entirely into biomass, CO_2, H_2, and organic acids, we determined metabolic fluxes in wild-type and NifA* cells by use of ^{13}C-labeled fumarate, succinate, and butyrate and ^{13}C-labeled butyrate with unlabeled $NaHCO_3$. We determined the metabolic fluxes using measurements of organic acids and CO_2, the *R. palustris* biomass composition (7), and the ^{13}C-labeling patterns obtained from proteinaceous amino acids (see Tables S2 to S4 in the supplemental material). The labeling patterns that

TABLE 2 Conversion of substrates to biomass, CO_2, organic acids, and H_2 by *R. palustris* during exponential growth[a]

	Doubling time (h)		Yield (mol/mol organic C consumed)[b]											
			Biomass[c]		CO_2		Organic acids[d]		H_2		% C recovery[e]		% electron recovery[e]	
Substrate	WT	NifA*	WT	NifA*	WT	NifA*	WT	NifA*	WT	NifA*	WT	NifA*	WT	NifA*
Fumarate	10.6 ± 1.0[f]	13.2 ± 0.8[f]	62 ± 3	47 ± 2	28 ± 1	29 ± 1	12 ± 2	30 ± 3		18 ± 3[g]	101 ± 5	106 ± 2	104 ± 6	109 ± 3
Succinate	6.5 ± 0.4	8.2 ± 0.5	82 ± 3	67 ± 3	15 ± 1	27 ± 1	0.1 ± 0.0	0.1 ± 0.0		23 ± 1	97 ± 4	94 ± 3	106 ± 4	99 ± 3
Acetate[h]	8.4 ± 0.6	9.4 ± 0.6	88 ± 8	79 ± 4	6 ± 1	17 ± 2	0	0		21 ± 3	93 ± 8	96 ± 5	98 ± 9	99 ± 5
Butyrate-HCO_3^-	8.6 ± 0.4	10.7 ± 1.0	83 ± 6	84 ± 6	−18 ± 4	−11 ± 3	28 ± 3	23 ± 5		11 ± 3	94 ± 5	97 ± 5	97 ± 5	99 ± 8
Butyrate	No growth	32.4 ± 7.6		67 ± 12		6 ± 1		24 ± 2		41 ± 10		97 ± 14		96 ± 15

[a] Unlabeled cultures were grown in minimal medium with NH_4^+ as the nitrogen source. Values are averages from 3 to 5 biological replicates ± SD based on samples taken during early exponential growth.

[b] Values are normalized for organic C consumed to account for acetate having two carbon atoms, whereas the other substrates have four. Negative signs indicate that there was a net consumption of CO_2, which was made possible by the $NaHCO_3$ supplement.

[c] Moles of biomass were determined from the *R. palustris* 42OL elemental composition (25): $CH_{1.8}N_{0.18}O_{0.38}$ (mole weight, 22.426 g/mol).

[d] Malate was excreted during growth on fumarate, fumarate was excreted during growth on succinate, and acetate was excreted during growth on butyrate.

[e] The percentage of organic carbon and electrons consumed that were observed in products. The sum of the values in biomass, CO_2, and organic acids would equal 100 for full carbon recovery. Electron recovery was based on available hydrogen as described previously (7, 26).

[f] Growth rates during the second growth phase on fumarate.

[g] Calculated by grouping fumarate and malate as a single metabolite [i.e., dH_2/d(fumarate + malate) × 100/4 carbon atoms]. The H_2 yield from fumarate consumed alone would give a value of 12 ± 2.

[h] The acetate data were previously published (7).

were informative for determining specific fluxes for [1,4-^{13}C]fumarate and [1,4-^{13}C]succinate were essentially the same as those described for [1-^{13}C]acetate (7). For example, fully labeled serine was a pattern uniquely generated by the Calvin cycle as it assimilated $^{13}CO_2$ originating from the ^{13}C-carboxyl groups of the organic substrate. Conversely, metabolism of [2,4-^{13}C]butyrate resulted in the liberation of unlabeled carboxyl groups, such that the informative labeling patterns were the inverses of those obtained when the carboxyl groups were labeled (e.g., the Calvin cycle uniquely generated fully unlabeled serine).

The central metabolic flux maps obtained for the wild type and the NifA* strain grown on the different substrates and previously reported flux maps for cells grown on acetate (7) are shown in Fig. 1 (values and confidence intervals, including those for biosynthetic fluxes, are in Tables S5 to S8 in the supplemental material). As was found with growth on acetate, most wild-type fluxes appeared to be distributed to satisfy the demands for biosynthetic fluxes except for flux through the Calvin cycle. Tricarboxylic acid (TCA) cycle fluxes were generally very low unless a TCA cycle reaction was needed to metabolize substrate to generate biosynthetic precursors. As expected, acetate and butyrate were mainly assimilated via the glyoxylate shunt, whereas there was no glyoxylate shunt flux during growth on fumarate or succinate.

Previously, we reported that only half of the reduced electron carriers generated during growth on acetate were oxidized in biosynthetic reactions and that, in the absence of H_2 production, the Calvin cycle played a critical role by oxidizing most of the remaining reduced electron carriers in the cell (7). To sustain this large Calvin cycle flux, *R. palustris* refixed nearly 70% of the CO_2 that was liberated during the oxidation of acetate. This was the only source of CO_2 in the cultures. Succinate and fumarate are more oxidized than acetate and *R. palustris* biomass, whereas butyrate is more reduced (Table 1). Thus, one would expect the Calvin cycle to play an increasingly important role as the substrate electron content increases. Our flux data show that wild-type cells converted a significant percentage of all metabolized substrates to CO_2 (Table 3) and then refixed various amounts of this CO_2 via the Calvin cycle (Table 3), allowing for oxidation of NADH by the Calvin cycle enzyme, glyceraldehyde 3-phosphate dehydrogenase (GAPDH) (Calvin flux in Fig. 2A). Figure 2 shows the contribution of various pathways and reactions that either oxidize (positive bars above the *x* axis) or reduce (negative bars below the *x* axis) electron carriers for the two strains. For all substrates, the flux distributions describe systems that are within 10% of being electron balanced, except for NifA* fluxes on fumarate. For achieving electron balance, we assumed that *R. palustris* uses mechanisms such as transhydrogenase to transfer electrons between specific carriers as needed (e.g., NADH + $NADP^+ \rightarrow NAD^+$ + NADPH). Indeed, all flux maps suggested that between 74% (NifA* strain on fumarate) and 89% (wild type on acetate) of the NADPH requirement was met by a transhydrogenase-like reaction. Generally, the total flux that reduced electron carriers was less during growth on more-oxidized substrates (Fig. 2A, collective negative bar). However, in all cases, the wild-type Calvin cycle flux was estimated to oxidize large proportions of the electron carriers, specifically, 38% on fumarate, 51% on succinate, 43% on acetate, and 55% on butyrate with $NaHCO_3$ (Fig. 2A). This electron carrier oxidation was essential, because a RuBisCO-deleted (ΔRuBisCO) strain (CGA669; wild-type *R. palustris* with both sets of RuBisCO genes deleted) did not grow on any of the substrates under the same growth conditions. Therefore, even on substrates as oxidized as fumarate, a large proportion of reduced electron carriers cannot be used for biosynthesis and must be oxidized via the Calvin cycle.

Biosynthetic precursor demands and pathway constraints influence the requirement for Calvin cycle activity. Although the Calvin cycle oxidized a large proportion of electron carriers in wild-type *R. palustris* for each substrate, the actual Calvin cycle flux values were still generally lower during growth on more-oxidized substrates than on more-reduced substrates (Fig. 2A). As an exception to this trend, wild-type *R. palustris* grown on succinate was estimated to involve 1.2-fold-higher GAPDH and RuBisCO fluxes than that grown on acetate, a more reduced substrate. The route taken to generate acetyl-coenzyme A (CoA) can explain the large Calvin cycle flux on succinate relative to that on acetate. *R. palustris* generates acetyl-CoA as a major biosynthetic precursor to biomass components that make up over 20% of the

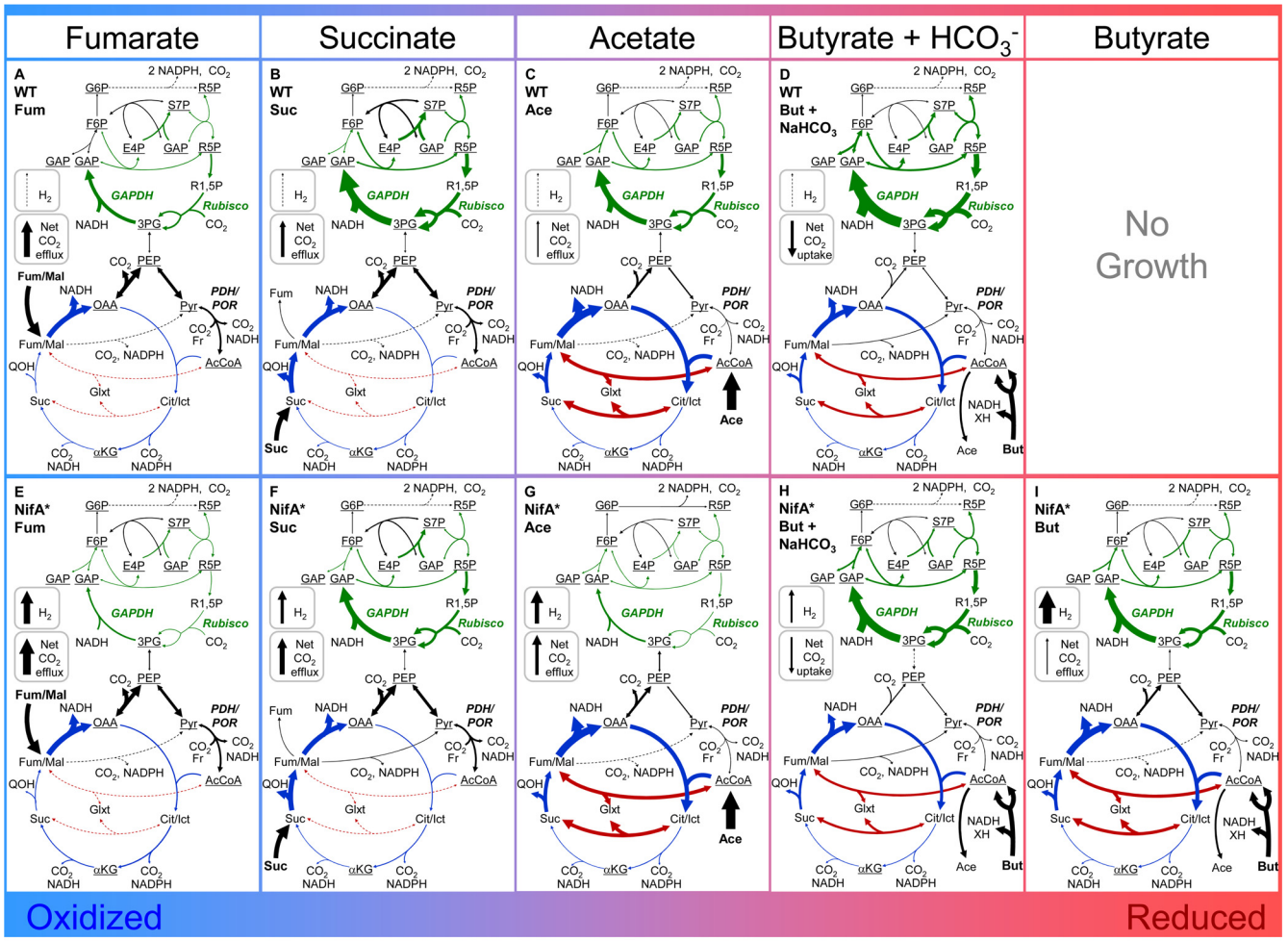

FIG 1 Central metabolic fluxes in non-H_2-producing wild-type cells and H_2-producing NifA* cells. The metabolic network is based on the *R. palustris* genome sequence and simplified by grouping reactions that do not affect labeling patterns. The Calvin cycle is highlighted in green, the TCA cycle in blue, and the glyoxylate shunt in red. Underlined metabolites indicate starting points for biosynthetic reactions that are not shown. The complete network was described previously (7) and is described in Table S1 in the supplemental material. Net flux magnitude, as mole percentage of the substrate uptake flux, is indicated by arrow thickness. The value for acetate uptake was normalized to 100, whereas the values for 4-carbon substrates were normalized to 50 to account for the different carbon contents. Net flux direction is indicated by an enlarged arrowhead for those fluxes assumed to be bidirectional. Wild-type flux distributions are shown along the top for fumarate (A), succinate (B), acetate (C), and butyrate with $NaHCO_3$ (D). NifA* flux distributions during H_2 production are shown along the bottom for fumarate (E), succinate (F), acetate (G), butyrate with $NaHCO_3$ (H), and butyrate with NaCl (I). Flux distributions for acetate were previously reported (7). All fluxes are based on samples taken during early exponential growth. Reactions: GAPDH, glyceraldehyde-3-phosphate dehydrogenase; PDH/POR, pyruvate dehydrogenase/pyruvate ferredoxin oxidoreductase; RuBisCO, ribulose 1,5-bisphosphate carboxylase. Metabolites: 3PG, 3-phosphoglycerate; AcCoA, acetyl coenzyme A; αKG, α-ketoglutarate; Cit/Icit, citrate/isocitrate; E4P, erythrose 4-phosphate; F6P, fructose 6-phosphate; Fum/Mal, fumarate/malate; Fr, ferredoxin; G6P, glucose-6-phosphate; GAP, glyceraldehyde 3-phosphate; Glxt, glyoxylate; OAA, oxaloacetate; PEP, phosphoenolpyruvate; Pyr, pyruvate; QOH, quinol; R5P, pentose phosphates; R1,5P, ribulose 1,5-bisphosphate; S7P, sedoheptulose 7-phosphate; Suc, succinate; XH, unknown reduced electron carrier.

dry cell weight (7). When acetate is taken up, it is converted directly to acetyl-CoA. However, succinate is processed through the TCA cycle and decarboxylated twice to produce acetyl-CoA (Fig. 1). As a consequence, growth on succinate involved a relatively high forward flux through pyruvate dehydrogenase and/or pyruvate ferredoxin oxidoreductase (PDH/POR), which reduces electron carriers (Fig. 1 and 2A). The high forward PDH/POR flux during growth on succinate contributed to a total flux through reactions that reduce electron carriers that was similar to that observed during growth on acetate (Fig. 2A). A second consequence of the route from succinate to acetyl-CoA is the loss of carbon as CO_2. Wild-type conversion of substrate to CO_2 was 1.7-fold higher during growth on succinate than during that on acetate, and the net CO_2 yield was three times higher (Table 3). This high CO_2 yield from succinate resulted in less carbon for biosynthesis. Therefore, biosynthetic reactions during growth on succinate do not require as many reducing equivalents as those during growth on acetate (46% versus 52% of total electron carrier oxidizing flux, respectively). To counter the extra electron carrier reduction by PDH/POR and the lack of electron carrier oxidation by biosynthesis, the Calvin cycle refixed about half of the CO_2 produced from succinate oxidation (Table 3 and Fig. 2A).

Whereas succinate and acetate take different routes to biosynthetic precursors, compounds that enter metabolism at similar

TABLE 3 CO_2 produced by various metabolic reactions and refixed by RuBisCO[a]

Substrate	% of substrate converted to CO_2 (relative to amt of substrate consumed)		% of CO_2 refixed by Calvin cycle (relative to amt of substrate converted to CO_2)		Net CO_2 yield (% relative to amt of substrate consumed)	
	WT	NifA*	WT	NifA*	WT	NifA*
Fumarate[b]	40 ± 4	44 ± 4	21 ± 9	6 ± 1	32 ± 2	42 ± 2
Succinate	37 ± 3	40 ± 2	49 ± 7	30 ± 5	19 ± 2	28 ± 2
Acetate[c]	22 ± 2	23 ± 1	68 ± 11	13 ± 3	6 ± 1	18 ± 1
Butyrate-HCO_3^-	16 ± 1	15 ± 3	180 ± 16[e]	149 ± 36[e]	−16 ± 1[f]	−10 ± 3[f]
Butyrate[d]		23 ± 3		76 ± 17		6 ± 1

[a] Average values with 90% confidence intervals were derived from the fluxes shown in Fig. 1. Minor variations between CO_2 yields in Tables 2 and 3 are due to changes made by the fitting algorithm to find the most likely set of fluxes to explain all of the data.

[b] All values were calculated by grouping malate and fumarate as a single pool. This grouping results in different CO_2 yields between Tables 2 and 3, because the CO_2 yields in Table 2 were normalized to fumarate alone so that the amount of malate produced could also be reported. If fumarate and malate were grouped in Table 2, the CO_2 yields would be the same as those reported in Table 3.

[c] The acetate data were previously published (7).

[d] Wild-type cells do not grow without the $NaHCO_3$ supplement.

[e] One hundred percent of the butyrate converted to CO_2 was refixed along with CO_2 from the $NaHCO_3$ supplement.

[f] The negative values indicate that there was a net uptake of CO_2 from the $NaHCO_3$.

locations, such as succinate and fumarate, result in Calvin cycle fluxes that more closely reflect the substrate oxidation state. Fumarate was processed similarly to succinate to reach biosynthetic precursors, including a relatively large flux through PDH/POR (Fig. 1). The similar metabolic flux distributions are reflected in the similar levels of substrate converted to CO_2 (Table 3). However, since fumarate is not processed by succinate dehydrogenase (Fig. 1) (Suc → Fum/Mal), there was less total reduction of electron carriers than during growth on succinate (Fig. 2A). Correspondingly, the wild-type Calvin cycle (GAPDH) flux that recycles oxidized electron carriers was about half of that obtained during growth on succinate (Fig. 1 and 2A). The lower RuBisCO flux recaptured only 21% of the CO_2, resulting in 1.8-fold-higher net CO_2 yield during growth on fumarate than during that on succinate (Fig. 1 and Table 3).

Similarly, acetate and butyrate are both processed through acetyl-CoA and the glyoxylate shunt. However, degradation of butyrate to two acetyl-CoA molecules through β-oxidation results in two reduced electron carriers (Fig. 1). As a result, the total flux that reduces electron carriers was nearly 1.5 times higher during growth of wild-type *R. palustris* on butyrate with $NaHCO_3$ than during that on acetate (Fig. 2A). To compensate, GAPDH flux was 1.8-fold higher during growth on butyrate with $NaHCO_3$ than during that on acetate (Fig. 1). As observed during growth on acetate (7), growth on butyrate was associated with a small amount of electron carrier oxidation by a proposed POR flux from

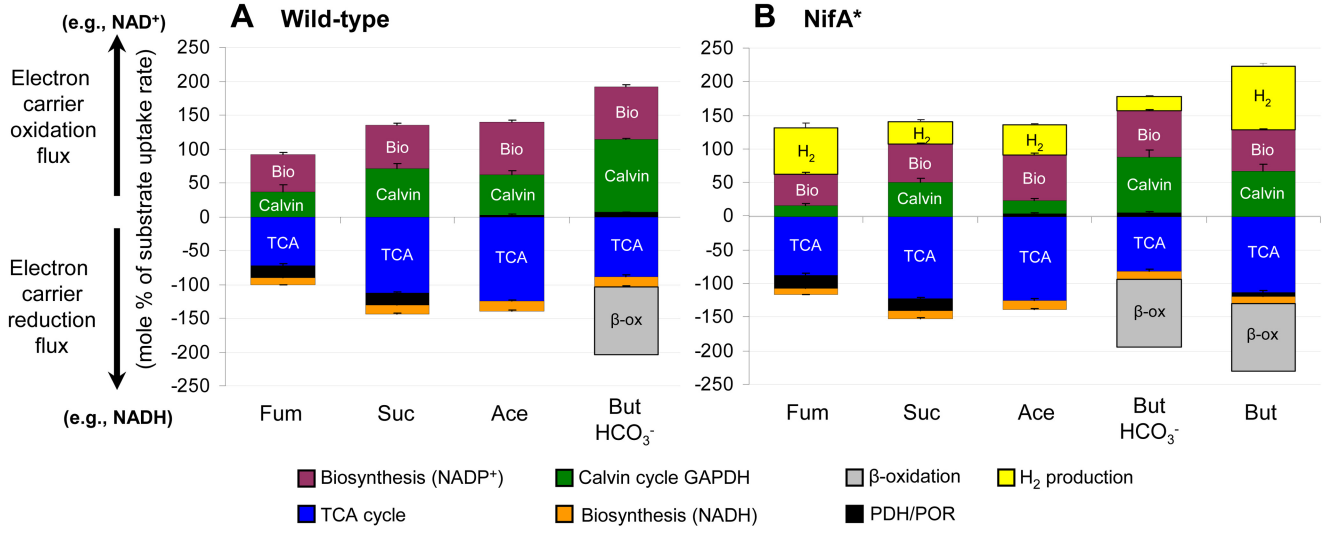

FIG 2 Metabolic flux distributions balance electrons. The positive bars above the *x* axis represent fluxes through reactions that oxidize electron carriers, whereas the negative bars below the *x* axis bars represent fluxes through reactions that reduce electron carriers (based on values in Fig. 1). Electron balance is indicated when the collective bar sizes on opposing sides of the graph are equal. Flux distributions from all substrates for both wild-type R. *palustris* (A) and the NifA* strain (B) achieved electron balance within 10% except for the NifA* strain on fumarate (electron carrier-oxidizing flux was 113% of electron carrier-reducing flux). β-Oxidation is the pathway by which butyrate is converted into two acetyl-CoA molecules. Biosynthesis ($NADP^+$) and biosynthesis (NADH) reflect the total NADPH oxidation and NAD^+ reduction, respectively, by fluxes through biosynthetic reactions. Data from acetate were reported previously (7).

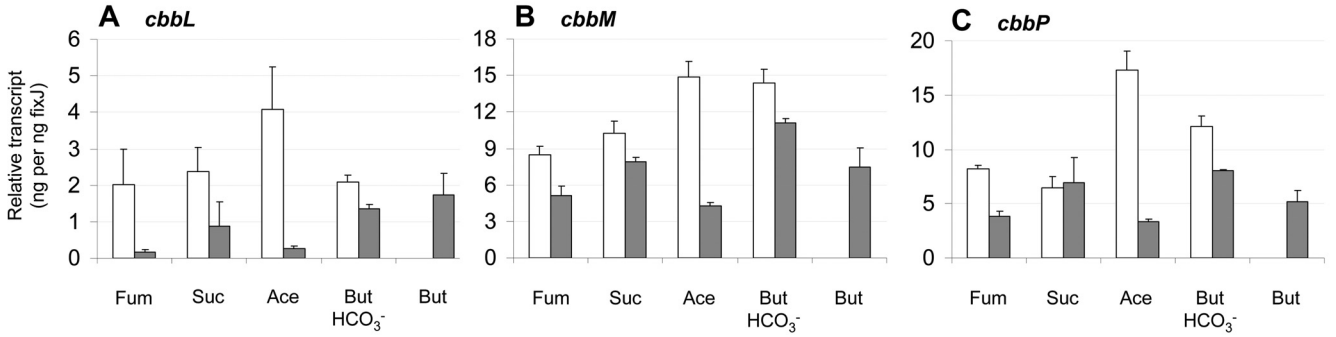

FIG 3 H_2 production results in lower Calvin cycle gene expression. Transcript levels are shown relative to those for *fixJ*. Absolute transcript levels for Calvin cycle genes and *fixJ* are shown in Fig. S1 in the supplemental material. Data are averages from duplicate cultures, with error bars representing the range. White bars, wild type (no H_2 produced); gray bars, NifA* strain (H_2 produced). (A) *cbbL*, encoding the RuBisCO type I large subunit; (B) *cbbM*, encoding RuBisCO type II; and (C) *cbbP*, encoding phosphoribulokinase. Data from acetate were reported previously (7).

acetyl-CoA to pyruvate (Fig. 1). Even though growth of wild-type *R. palustris* on butyrate resulted in net CO_2 fixation, our flux map indicates that 16% of butyrate was converted to CO_2 (Table 3). All of this CO_2 from butyrate oxidation, along with CO_2 from the added $NaHCO_3$, was fixed by RuBisCO and the proposed POR flux (Table 3). Taken together, our results illustrate how the point at which a substrate enters metabolism and the route taken to reach biosynthetic precursors can influence the amount of electron carrier that is reduced, which in turn affects the amount of CO_2 fixed or, as described in the next sections, H_2 produced.

Calvin cycle fluxes decrease in response to H_2 production. Using the NifA* strain, we examined the effect of H_2 production on metabolic fluxes for the four different substrates. We also obtained a flux map for cells grown on butyrate without added $NaHCO_3$, since unlike wild-type *R. palustris*, the NifA* strain grows under these conditions. As can be seen in Fig. 1, the flux maps look very similar for non-H_2-producing (wild-type) and H_2-producing (NifA*) cells except for the Calvin cycle fluxes, which are lower in H_2-producing cells. During growth on acetate (7), the decrease in Calvin cycle flux made nearly 90% of the electrons for the H_2 produced available, with the rest being accounted for by decreased use of reducing equivalents for biosynthesis (compare Fig. 2A and B). There is less need for reducing equivalents for biosynthesis by the NifA* strain because more electrons are lost as H_2 and fewer are used for fixing CO_2 into biomass, as indicated by the lower biomass yields for the NifA* strain (Table 2). Similar to what was observed on acetate, the decrease in Calvin cycle flux during growth of the NifA* strain on butyrate with $NaHCO_3$ was enough to account for all of the H_2 produced (Fig. 2). For the other substrates, the decrease in Calvin cycle flux did not make as large a contribution, accounting for 29%, 64%, and 43% of the H_2 production during growth on fumarate, succinate, and butyrate, respectively. Nevertheless, in each case the decrease in Calvin cycle GAPDH flux was the largest single contributor of electrons for H_2 production. This cannot be said with absolute certainty for growth on fumarate, as 36% of the electrons needed to explain the amount of H_2 observed were unaccounted for. Unlike what was observed on acetate, increased TCA cycle fluxes contributed some electrons for H_2 production during growth on fumarate, succinate, and especially butyrate without $NaHCO_3$ (Fig. 2). This is not evident from a visual inspection of the flux maps in Fig. 1, because several reactions contribute to the overall TCA cycle flux.

H_2 production accounted for one-third of electron carrier oxidation in the NifA* strain during growth on acetate, compensating for the low Calvin cycle flux (Fig. 2B) (7). However, on other carbon sources, like succinate and butyrate, the Calvin cycle still oxidized a large proportion of the reduced electron carriers, even when nitrogenase was induced and available to form H_2 as an electron sink (Fig. 2B). For example, the NifA* CO_2-fixing RuBisCO flux was still 75% of the wild-type value during growth on butyrate with $NaHCO_3$ (Fig. 2). The importance of CO_2 fixation during growth on butyrate was further exemplified by our analysis of cells grown in the absence of $NaHCO_3$. Without $NaHCO_3$, the NifA* strain grew about 3 times more slowly on butyrate (Table 2) and relied heavily on the Calvin cycle to oxidize electron carriers, using CO_2 released endogenously from butyrate itself (Table 3).

As we observed with acetate (7), the decrease in Calvin cycle flux was accompanied by a decrease in the transcription of Calvin cycle genes during growth on the other substrates (Fig. 3). In parallel with the flux data, decreases in Calvin cycle gene expression were generally not as drastic as those observed during growth on acetate, especially for *cbbM* (RuBisCO type II) and *cbbP* (phosphoribulokinase).

H_2 yields increase when Calvin cycle flux is blocked by mutation. Since a significant percentage of the reducing equivalents generated by the oxidation of each substrate were used for CO_2 fixation, even during H_2 production (Fig. 2), the Calvin cycle represents an attractive, nonessential target to mutate to force more electrons towards H_2. To test this, we grew the NifA* strain and a NifA* ΔRuBisCO strain (CGA679; NifA* strain with both sets of RuBisCO genes deleted) side by side on the four substrates and compared the H_2 yields. For each substrate, the H_2 yield from the NifA* ΔRuBisCO strain was higher than that from the NifA* parent (Fig. 4). When RuBisCO type I was expressed from a plasmid vector in the NifA* ΔRuBisCO strain, the H_2 yields were similar to or lower than those of the parent. Introduction of an empty vector into this strain has no effect on H_2 production. The NifA* parent still relied heavily on the Calvin cycle during growth on succinate and butyrate (Fig. 2B). Thus, we expected a larger increase in the H_2 yields for the ΔRuBisCO strain on succinate and

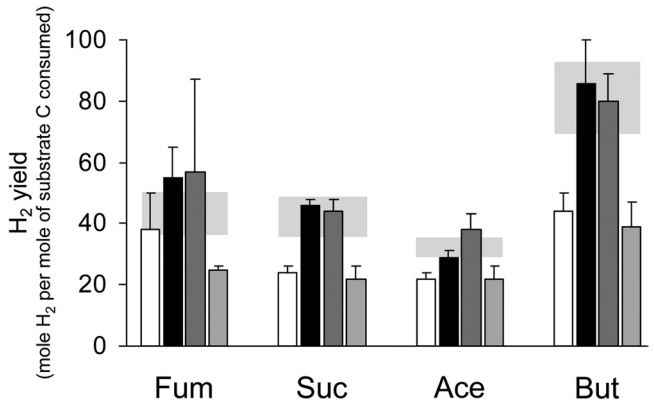

FIG 4 The H_2 yield increases when Calvin cycle flux is blocked by mutation. Hydrogen yields from a NifA* ΔRuBisCO strain that is incapable of Calvin cycle flux due to the deletion of all genes encoding RuBisCO enzymes (CGA679; black bars) were higher than those from the NifA* parent (CGA676; white bars). Including pBBPgdh as a vector control (dark gray bars) does not affect H_2 yields, but expressing RuBisCO type I from pBBP*cbbLSX* in the ΔRuBisCO strain results in H_2 yields similar to those from the NifA* parent (light gray bars). Averages from 3 to 10 biological replicates are shown with 90% confidence intervals. Hydrogen yields from acetate were reported previously (7). The shaded boxes show the H_2 yield ranges, based on 90% confidence intervals, expected if all electrons associated with Calvin cycle flux in the NifA* parent were diverted to H_2 production.

butyrate than on acetate. Indeed, the H_2 yields on succinate and butyrate increased about 2-fold, compared to 1.3-fold during growth on acetate. In general, our data indicate that the Calvin cycle flux of a NifA* strain can be used to predict the H_2 yield of a NifA* ΔRuBisCO strain (Fig. 4). However, the increase in the H_2 yield for fumarate was unexpectedly high, as the parent NifA* strain was estimated to have low Calvin cycle flux (Fig. 2B). As we observed previously (7), during growth on acetate, the NifA* ΔRuBisCO strain grew more slowly than the NifA* parent on all substrates (the NifA* ΔRuBisCO strain growth rate ranged from 0.6 [fumarate] to 0.9 [acetate] times that of the parent growth rate).

DISCUSSION

Balancing electrons is a challenge for a PNSB like *R. palustris* growing photoheterotrophically because energy is obtained by cycling electrons in cyclic photophosphorylation and not by transferring them to a terminal electron acceptor. During this mode of growth, reducing equivalents that are generated during the oxidation of an organic carbon source, but which cannot be put towards biosynthesis, can be used to fix CO_2 via the Calvin cycle or released as H_2 via nitrogenase. Using ^{13}C metabolic flux analysis, we found that in the absence of H_2 production, a significant proportion of electron carriers (38 to 55%) were oxidized by the Calvin cycle regardless of the substrate oxidation state. It is interesting that fluxes through the oxidative pentose phosphate pathway (Fig. 1) (G6P → R5P + CO_2), the TCA cycle, and PDH/POR were very low for all substrates unless a substrate needed to be processed by one of these pathways to make biosynthetic precursors (Fig. 1). Given the challenge associated with photoheterotrophic growth in maintaining electron balance, the low flux through these reactions makes sense in order to maintain a low rate of electron carrier reduction.

In some cases, the biochemical constraints of a metabolic network affect the overall need for electron carrier oxidation, and thereby the amount of CO_2 fixed or H_2 produced, by dictating the route that must be taken towards biosynthetic precursors. Specifically, the route succinate took to generate acetyl-CoA produced a level of reducing equivalents similar to that produced by growth on a more reduced substrate, acetate (Fig. 2). This led to Calvin cycle fluxes and H_2 yields that were unexpectedly high with succinate relative to those with acetate. This effect is expected to be more pronounced when bacteria that have different metabolic inventories are compared. For example, *R. sphaeroides* assimilates acetate using the reductive ethylmalonyl-CoA pathway (14), unlike *R. palustris*, which uses the oxidative glyoxylate shunt. It was recently shown that the ethylmalonyl-CoA pathway oxidizes enough electron carriers during acetate assimilation such that the Calvin cycle and H_2 production were dispensable for photoheterotrophic growth (15). Given the obligate nature of this reductive pathway in *R. sphaeroides* for growth on acetate, one would expect that H_2 yields would be lower than those of a bacterium using the glyoxylate shunt.

To produce H_2, the NifA* strain shifted electrons away from CO_2 fixation to H_2 production, such that the necessary electron carrier oxidation was shared by the two activities. However, the Calvin cycle flux decreased to different extents, depending on the substrate (Fig. 1 and 2), and thereby affected the H_2 yield. We verified this by showing that a NifA* ΔRuBisCO strain that is incapable of Calvin cycle flux had higher H_2 yields than the NifA* parent (Fig. 4). Preventing Calvin cycle flux in a *Rhodospirillum rubrum* NifA* mutant was also recently shown to improve the H_2 yield (11). It is not clear why there was a greater decrease in Calvin cycle flux in response to H_2 production during growth on acetate than during growth on other substrates. One possibility is that the higher levels of CO_2 produced during growth on fumarate and succinate and the addition of $NaHCO_3$ to the butyrate cultures allowed for greater participation of RuBisCO type II, which has a low affinity for CO_2.

There are other factors that can also affect the H_2 yield. It is well documented that excretion of organic acids or synthesis of electron-rich polymers such as polyhydroxybutyrate can influence the H_2 yield (5, 12). Under our growth conditions, organic acid excretion does not affect the final H_2 yield, since excreted compounds were eventually consumed. Changes to polyhydroxybutyrate and other biomass components (in addition to the potential effects of biphasic growth on labeling patterns) could help explain why we were unable to account for 36% of the electrons in H_2 produced from fumarate by the NifA* strain. We assumed that the biomass composition on fumarate was the same as that observed for growth on succinate and acetate (7). It was also suggested that the free energy of a substrate can influence the H_2 yield from PNSB (5). However, our results (and data from others) do not show the same correlation (see Fig. S2 in the supplemental material). Rather, there appears to be a large variability in H_2 yields among PNSB (Fig. S2), barring any influence from the different experimental procedures used. In this paper, we identified two metabolic factors that help explain variable H_2 yields among different PNSB: (i) the route taken to generate biosynthetic precursors and (ii) the amount of competing Calvin cycle flux.

TABLE 4 Strains and plasmids used

Strain or plasmid	Genotype or phenotype	Reference
R. palustris strains		
CGA009	Wild-type strain; spontaneous Cm^r derivative of CGA001	17
CGA676	NifA*; produces H_2 in the presence of NH_4^+	7
CGA669	Δ*cbbLS*::Km^r Δ*cbbM* mutant of CGA009	7
CGA679	Δ*cbbLS*::Km^r Δ*cbbM* mutant of CGA676	7
Plasmids		
pBBPgdh	Gm^r; pBBR1MCS-5 with RPA0944 promoter between KpnI and XhoI sites	7
pBBP*cbbLSX*	Gm^r; *cbbLSX* with native ribosomal binding site cloned into pBBPgdh	7

MATERIALS AND METHODS

Chemicals, bacteria, and culture conditions. [1,4-^{13}C]fumaric acid and [1,4-^{13}C]succinic acid were purchased from Cambridge Isotope Laboratories (Andover, MA) and were neutralized with NaOH prior to use. Sodium [2,4-^{13}C]butyrate was purchased from Sigma-Aldrich (St. Louis, MO). All other chemicals were purchased from either Sigma-Aldrich or Fisher Scientific (Pittsburg, PA). All experiments were conducted on *R. palustris* wild-type strain CGA009 or its derivatives and are listed in Table 4. CGA009 is defective in uptake hydrogenase activity (16). CGA676 is a NifA* strain derived from CGA009 that constitutively produces H_2 via nitrogenase (7) and was used to examine the effects of H_2 production in media containing NH_4^+. *R. palustris* strains were grown anaerobically in 16.5-ml volumes of defined mineral medium (17) containing 7.5 mM $(NH_4)_2SO_4$ under an argon headspace (i.e., PM medium) in sealed 27-ml tubes in front of a 60-W light bulb at 30°C. Organic acids were supplied at a final concentration of 40 mM carbon (e.g., 10 mM succinate or 20 mM acetate). Cultures grown with butyrate were supplemented with either $NaHCO_3$ or NaCl to give a final concentration of 10 mM. $NaHCO_3$ stock solutions were prepared as described previously (18, 19).

Analytical techniques. Organic acids were quantified using a Varian high-performance liquid chromatograph (HPLC) with a UV detector at 210 nm as described previously (18). H_2 was quantified using a gas chromatograph with a molecular sieve 5A column (Sigma-Aldrich) as described previously (20). CO_2 was quantified by gas chromatography as described previously (7). All samples were taken during early exponential growth (i.e., <0.5 OD_{660} units).

^{13}C-labeling experiments and metabolic flux analysis. Three or four biological replicates each of CGA009 or CGA676 were cultured with 100% ^{13}C-labeled substrate, subcultured, and harvested during the early exponential growth phase (OD_{660}, 0.35 to 0.45) as described previously (7). Cultures were periodically sampled to quantify substrate consumption, H_2 production, organic acid excretion, and biomass formation. ^{13}C-labeled amino acids were obtained from the cell pellets by acid hydrolysis and derivatized and mass isotopomer distributions determined using gas chromatography-mass spectrometry (GC-MS) as described previously (21). Mass isotopomer distributions were corrected for natural abundances of all atoms except for the carbon atoms in amino acid backbones using previously described software (22). Corrected amino acid mass isotopomer distributions and extracellular flux measurements (i.e., organic acid excretion, CO_2 production, and biosynthetic fluxes based on the *R. palustris* biomass composition [7]) were used with a metabolic model (see Table S1 in the supplemental material) based on the *R. palustris* genome sequence (7) to solve intermediary metabolic fluxes using previously described software (23). Confidence intervals (90%) for individual fluxes were determined as described previously (24). No redox constraints were used in determining metabolic flux distributions. In our metabolic model, fumarate and malate were treated as a single pool to account for simultaneous production and consumption of fumarate and malate (see Results). Since fumarate and malate have the same oxidation state, grouping these two metabolites did not affect our electron balance calculations. The *R. palustris* biomass compositions were based on data collected for CGA009 and CGA676 grown on either succinate or acetate in the presence of NH_4^+ (7) and were assumed to be similar for growth on fumarate and butyrate for this study.

Electron balance and H_2 yield calculations. Electron balance was assessed by two different methods. The first method used extracellular measurements to determine the sum of the electrons in H_2, organic acids, and biomass produced as a fraction of electrons in substrate consumed. *R. palustris* biomass was assumed to have 4.5 electrons per mole of carbon and was determined using a standard curve relating OD_{660} to dry cell weight and an assumed biomass composition of $CH_{1.8}N_{0.18}O_{0.38}$ (25) as described previously (7). The second method used intermediary flux values obtained from ^{13}C-labeling experiments to determine the sum of fluxes through reactions that oxidize electron carriers as a fraction of the sum of fluxes that reduce electron carriers. For this calculation, we did not distinguish between different types of electron carriers, as we assumed that *R. palustris* uses transhydrogenase to transfer electrons between different carriers (7).

qRT-PCR analysis. RNA was purified from cultures in early exponential growth (0.3 to 0.5 OD_{660} units) using an RNeasy minikit (Qiagen, Valencia, CA), and genes encoding the large subunit of RuBisCO type I (*cbbL*), RuBisCO type II (*cbbM*), and phosphoribulokinase (*cbbP*) were used to assess Calvin cycle gene expression by quantitative reverse transcription-PCR (qRT-PCR) as described previously (7). Further details are provided in Fig. S1 in the supplemental material.

ACKNOWLEDGMENTS

This research was supported by the Division of Chemical Sciences, Geosciences, and Biosciences, Office of Basic Energy Sciences, U.S. Department of Energy, through grant DE-FG02-05ER15707 and by the Office of Science (BER), U.S. Department of Energy, through grant DE-FG02-07ER64482.

We thank Yasuhiro Oda and Colin Lappala for assistance with RNA purification and qRT-PCR analysis and Martin Sadilek for assistance with gas chromatography-mass spectrometry analysis.

SUPPLEMENTAL MATERIAL

Supplemental material for this article may be found at http://mbio.asm.org/lookup/suppl/doi:10.1128/mBio.00323-10/-/DCSupplemental.

Figure S1, TIF file, 0.608 MB.
Figure S2, TIF file, 0.845 MB.
Table S1, PDF file, 0.134 MB.
Table S2, PDF file, 0.096 MB.
Table S3, PDF file, 0.096 MB.
Table S4, PDF file, 0.098 MB.
Table S5, PDF file, 0.111 MB.
Table S6, PDF file, 0.111 MB.
Table S7, PDF file, 0.111 MB.
Table S8, PDF file, 0.111 MB.

REFERENCES

1. **McKinlay JB, Harwood CS.** 2010. Photobiological production of hydrogen gas as a biofuel. Curr. Opin. Biotechnol. **21**:244–251.
2. **Hillmer P, Gest H.** 1977. H_2 metabolism in the photosynthetic bacterium *Rhodopseudomonas capsulata*: H_2 production by growing cultures. J. Bacteriol. **129**:724–731.
3. **Barbosa MJ, Rocha JM, Tramper J, Wijffels RH.** 2001. Acetate as a carbon source for hydrogen production by photosynthetic bacteria. J. Biotechnol. **85**:25–33.
4. **Rey FE, Heiniger EK, Harwood CS.** 2007. Redirection of metabolism for biological hydrogen production. Appl. Environ. Microbiol. **73**:1665–1671.
5. **Yilmaz L, et al.** 2010. Electron partitioning during light- and nutrient-

powered hydrogen production by *Rhodobacter sphaeroides*. Bioenerg. Res. **3**:55–66.
6. **Zou X, et al.** 2008. Identification and functional characterization of NifA variants that are independent of GlnB activation in the photosynthetic bacterium *Rhodospirillum rubrum*. Microbiology **154**:2689–2699.
7. **McKinlay JB, Harwood CS.** 2010. Carbon dioxide fixation as a central redox cofactor recycling mechanism in bacteria. Proc. Natl. Acad. Sci. U. S. A. **107**:11669–11675.
8. **Joshi HM, Tabita FR.** 1996. A global two component signal transduction system that integrates the control of photosynthesis, carbon dioxide assimilation, and nitrogen fixation. Proc. Natl. Acad. Sci. U. S. A. **93**: 14515–14520.
9. **Falcone DL, Tabita FR.** 1991. Expression of endogenous and foreign ribulose 1,5-bisphosphate carboxylase-oxygenase (Rubisco) genes in a Rubisco deletion mutant of *Rhodobacter sphaeroides*. J. Bacteriol. **173**: 2099–2108.
10. **Hallenbeck PL, Lerchen R, Hessler P, Kaplan S.** 1990. Roles of CfxA, CfxB, and external electron acceptors in regulation of ribulose 1,5-bisphosphate carboxylase/oxygenase expression in *Rhodobacter sphaeroides*. J. Bacteriol. **172**:1736–1748.
11. **Wang D, Zhang Y, Welch E, Li J, Roberts GP.** 2010. Elimination of Rubisco alters the regulation of nitrogenase activity and increases hydrogen production in *Rhodospirillum rubrum*. Int. J. Hydrogen Energy **35**: 7377–7385.
12. **Vincenzini M, Marchini A, Ena A, De Phillips R.** 1997. H_2 and poly-beta-hydroxybutyrate, two alternative chemicals from purple nonsulfur bacteria. Biotechnol. Lett. **19**:759–762.
13. **Muller FM.** 1933. On the metabolism of the purple sulfur bacteria in organic media. Arch. Microbiol. **4**:131–166.
14. **Erb TJ, et al.** 2007. Synthesis of C5-dicarboxylic acids from C2-units involving crotonyl-CoA carboxylase/reductase: the ethylmalonyl-CoA pathway. Proc. Natl. Acad. Sci. U. S. A. **104**:10631–10636.
15. **Laguna R, Tabita FR, Alber BE.** 2011. Acetate-dependent photoheterotrophic growth and the differential requirement for the Calvin-Benson-Bassham reductive pentose phosphate cycle in *Rhodobacter sphaeroides* and *Rhodopseudomonas palustris*. Arch. Microbiol. **193**:151–154.
16. **Rey FE, Oda Y, Harwood CS.** 2006. Regulation of uptake hydrogenase and effects of hydrogen utilization on gene expression in *Rhodopseudomonas palustris*. J. Bacteriol. **188**:6143–6152.
17. **Kim MK, Harwood CS.** 1991. Regulation of benzoate-CoA ligase in *Rhodopseudomonas palustris*. FEMS Microbiol. Lett. **83**:199–204.
18. **McKinlay JB, Zeikus JG, Vieille C.** 2005. Insights into *Actinobacillus succinogenes* fermentative metabolism in a chemically defined growth medium. Appl. Environ. Microbiol. **71**:6651–6656.
19. **Widdel F, Bak F.** 1992. Gram-negative mesophilic sulfate-reducing bacteria, p. 3358–3378. *In* Balows A, Trüper HG, Dworkin M, Harder W, Schleifer KH (ed), The prokaryotes, 2nd ed. Springer-Verlag, New York, NY.
20. **Huang JJ, Heiniger EK, McKinlay JB, Harwood CS.** 2010. Production of hydrogen gas from light and the inorganic electron donor thiosulfate by *Rhodopseudomonas palustris*. Appl. Environ. Microbiol. **76**:7717–7722.
21. **McKinlay JB, Shachar-Hill Y, Zeikus JG, Vieille C.** 2007. Determining *Actinobacillus succinogenes* metabolic pathways and fluxes by NMR and GC-MS analyses of ^{13}C-labeled metabolic product isotopomers. Metab. Eng. **9**:177–192.
22. **Wahl SA, Dauner M, Wiechert W.** 2004. New tools for mass isotopomer data evaluation in ^{13}C flux analysis: mass isotope correction, data consistency checking, and precursor relationships. Biotechnol. Bioeng. **85**: 259–268.
23. **Wiechert W, Möllney M, Petersen S, de Graaf AA.** 2001. A universal framework for ^{13}C metabolic flux analysis. Metab. Eng. **3**:265–283.
24. **Wiechert W, Siefke C, de Graaf AA, Marx A.** 1997. Bidirectional reaction steps in metabolic networks: II. Flux estimation and statistical analysis. Biotechnol. Bioeng. **55**:118–135.
25. **Carlozzi P, Sacchi A.** 2001. Biomass production and studies on *Rhodopseudomonas palustris* grown in an outdoor, temperature controlled, underwater tubular photobioreactor. J. Biotechnol. **88**:239–249.
26. **Gottschalk G.** 1986. Bacterial metabolism, 2nd ed. Springer-Verlag, New York, NY.